

Chapter 6

Biomechanical Modelling of the Brain for Neurosurgical Simulation and Neuroimage Registration



Karol Miller, Adam Wittek, Angus C. R. Tavnor, and Grand Roman Joldes

6.1 Introduction

During neurosurgery, the brain can deform significantly. Despite the enormous complexity of the brain (see Chap. 2), many aspects of its response can be reasonably described in purely mechanical terms, such as displacements, strains and stresses. Therefore the mechanical behaviour of the brain can be analysed using the established methods of continuum mechanics. In this chapter we discuss approaches to biomechanical modelling of the brain from the perspective of two distinct applications: neurosurgical simulation and neuroimage registration in image-guided surgery. These two challenging applications are described below.¹

6.1.1 Neurosurgical Simulation for Operation Planning, Surgeon Training and Skills Assessment

The goal of surgical simulation research is to model and simulate deformable materials for applications requiring real-time interaction. Medical applications for this include simulation-based training, skills assessment and operation planning.

¹Parts of this chapter were previously published in *International Journal for Numerical Methods in Biomedical Engineering*.

K. Miller (✉) · A. Wittek · A. C. R. Tavnor · G. R. Joldes
Intelligent Systems for Medicine Laboratory, School of Mechanical Engineering,
The University of Western Australia, Perth, WA, Australia
e-mail: karol.miller@uwa.edu.au

Surgical simulation systems are used to provide visual and haptic feedback to a surgeon or trainee. Various haptic interfaces for medical simulation are especially useful for training surgeons for minimally invasive procedures (laparoscopy/interventional radiology) and remote surgery using tele-operators. These systems must compute the deformation field within a soft organ and the interaction force between a surgical tool and the tissue to present visual and haptic feedback to the surgeon. Haptic feedback must be provided at frequencies of at least 500 Hz. From a solid-mechanics perspective, the problem involves large deformations, non-linear material properties and non-linear boundary conditions. Moreover, it requires extremely efficient solution algorithms to satisfy the stringent requirements of the frequency of haptic feedback. Thus, surgical simulation is a very challenging problem in solid mechanics.

When a simulator is intended to be used for surgeon training, a generic model developed from average organ geometry and material properties can be used in computations. However, when the intended application is for operation planning, the computational model must be patient-specific. This requirement adds to the difficulty of the problem – the question of how to rapidly generate patient-specific computational models still awaits a satisfactory answer [1].

6.1.2 Image Registration in Image-Guided Neurosurgery

One common element of most new therapeutic technologies, such as gene therapy, stimulators, focused radiation, lesion generation, nanotechnological devices, drug polymers, robotic surgery and robotic prosthetics, is that they have extremely localised areas of therapeutic effect. As a result, they have to be applied precisely in relation to the patient's current (i.e. intra-operative) anatomy, directly at the specific location of anatomic or functional abnormality [2]. Nakaji and Speltzer [3] list the 'accurate localisation of the target' as the first principle in modern neurosurgical approaches.

As only pre-operative anatomy of the patient is known precisely from medical images, usually magnetic resonance images (MRIs), it is now recognised that the ability to predict soft organ deformation (and therefore intra-operative anatomy) during the operation is the main problem in performing reliable surgery on soft organs. In the context of brain surgery, it is very important to be able to predict the effect of procedures on the position of pathologies and critical healthy areas in the brain. If displacements within the brain can be computed during the operation, then they can be used to warp pre-operative high-quality MR images so that they represent the current, intra-operative configuration of the brain; see Fig. 6.1.

The neuroimage registration problem involves large deformations, non-linear material properties and non-linear boundary conditions, as well as the difficult issue of generating patient-specific computational models. However, it is easier than the surgical simulation problem discussed above in two important ways. Firstly, we are interested in accurate computations of the displacement field only. Accuracy of

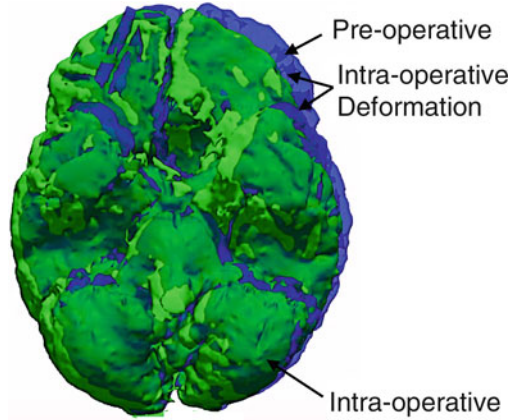


Fig. 6.1 Comparison of a brain surface determined from images acquired pre-operatively with the one determined intra-operatively from images acquired after craniotomy. Inferior (i.e. ‘bottom’) view. Pre-operative surface is semi-transparent. Deformation of the brain surface due to craniotomy is clearly visible. Intra-operative displacements of over 20 mm have been reported in medical literature [4]. Surfaces were determined from the images provided by the Department of Surgery, Brigham and Women’s Hospital (Harvard Medical School, Boston, Massachusetts, USA)

stress computations is not required. Secondly, the computations must be conducted intra-operatively, which practically means that the results should be available to an operating surgeon in less than 40 seconds [5–10]. This still requires computational efficiency but is much more easily satisfied than the 500 Hz haptic feedback frequency requirement for neurosurgical simulation.

Following the Introduction (Sect. 6.1), in Sect. 6.2 we describe difficulties in modelling geometry, boundary conditions, loading and material properties of the brain. In Sect. 6.3 we consider example applications in the area of computational radiology. Numerical algorithms devised to efficiently solve brain deformation behaviour models are described in Chaps. 10 and 11. We conclude this chapter with some reflections about the state of the field.

6.2 Biomechanics of the Brain: Modelling Issues

When considering approaches to modelling the brain, one should first determine whether the intended application is *generic* or *patient-specific* [110]. If the biomechanical model is intended for a generic application, for example, a neurosurgical simulator for surgeon training, the typical ‘average’ geometry and mechanical properties of an organ and tissues can be modelled. However, if a patient-specific model is required, for example, for operation planning, then clearly a ‘generic’ model is of limited utility, and patient-specific data must be incorporated into the model. The reader is warned here that the problem of how to generate patient-

specific biomechanical models quickly and reliably remains unresolved (see [1] and Chap. 7 for current attempts to address this issue using meshless methods). Another aspect worth considering is that for computational biomechanics to be accepted and beneficial in clinical practice, biomechanical computations must be seamlessly incorporated into the clinical work flow. This can only be achieved if these computations are conducted at least in close to real time (how to achieve this is discussed in Chap. 2; see also [11]).

In the remainder of this section, we will discuss the main modelling issues: geometry, boundary conditions, loading and tissue mechanical properties.

6.2.1 Geometry

Detailed geometric information is needed to define the domain in which the deformation field needs to be computed. Such information is provided by electronic brain atlases described in detail in Chap. 2 and is readily available as some atlases are web-based; see, e.g. Surgical Planning Laboratory Brain Atlas, Fig. 6.2.

In applications that do not require patient-specific data (such as neurosurgical simulators for education and training), the geometric information provided by these atlases is sufficient. However, other applications such as neurosurgical simulators for operation planning and image registration systems do require patient-specific data. Such data can be obtained from radiological images (e.g. see Fig. 6.3 and Chap. 3); however the quality is significantly inferior to the data available from anatomical atlases (see Chap. 2).

The accuracy of neurosurgery is typically not better than 1 mm [2]. Voxel size in high-quality pre-operative MR images is usually of similar magnitude. Therefore, we can conclude that patient-specific models of the brain geometry

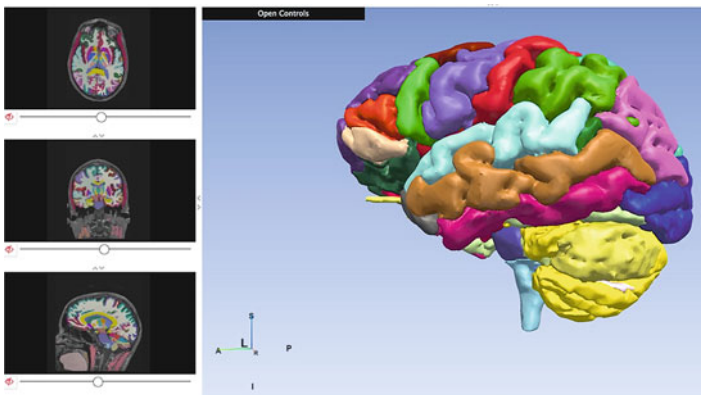
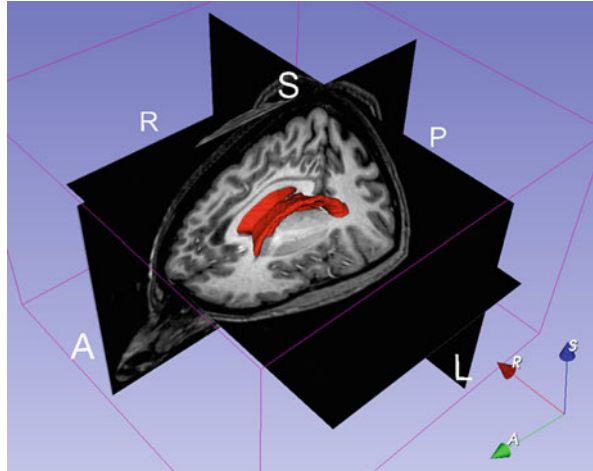


Fig. 6.2 Multimodality MRI-based atlas of the brain [13]

Fig. 6.3 3D magnetic resonance image presented as a triplanar cross-section. 3D rendering of ventricles is shown in red. Public domain software Slicer (www.slicer.org), developed by our collaborators from the Surgical Planning Laboratory, Harvard Medical School, was used to generate the image



can be constructed with approximately 1 mm accuracy and that higher accuracy is probably not required. One must then decide which brain structures should be explicitly included in the model and which omitted. As described in Chap. 2, anatomists recognise well over a thousand structures within the brain. However, very little is known about the relative mechanical properties of these structures. The ‘maps’ of brain regional mechanical properties from MR elastography are not yet reliable and are only valid for small strain (linear viscoelastic) [14, 15]. Therefore, even the most sophisticated models in current use by the scientific community typically only include brain parenchyma, ventricles, tumour (if present, for attempts to estimate tumour mechanical properties, see, e.g. [16–18].) and skull. I refer the reader to Chap. 4 of this book where mechanical properties of brain tissues are discussed in great detail.

A necessary step in constructing patient-specific models of brain geometry is medical image *segmentation*. Segmentation is a process that identifies different parts of the brain on the image; see Fig. 6.4.

Unfortunately, despite years of effort by the medical image analysis community, a generally accepted automatic segmentation method for brain MR images is not yet available. In practice, very laborious semi-automatic or manual methods are employed [10, 19]. It is clear that if one attempted to include many brain structures in the patient-specific biomechanical model, then one would need to identify them in the medical image and segment them. This would be a daunting task that at the time of writing does not appear to be practical.

On the other hand, when a generic application that does not require patient-specific data is considered, the 3D geometry of essentially all structures that might possibly be of interest can be imported from electronic brain atlases. For example, a hippocampus is often of interest, and its geometry and location can be clearly seen in Fig. 2.6 of Chap. 2.

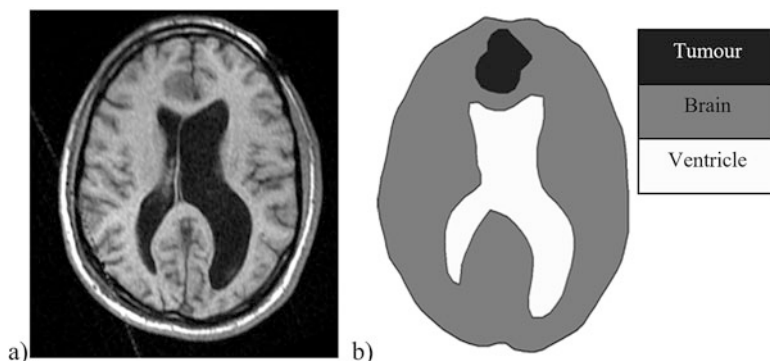


Fig. 6.4 (a) 2D slice of 3D brain MR volume; (b) segmented image. Such ‘hard’ segmentation is necessary for finite element mesh development

To develop a numerical model of brain biomechanics, it is necessary to create a computational grid, which in most practical cases is a finite element mesh (or a cloud of points required by a meshless method; see also Chaps. 5, 6, 10, and 11). Because of the stringent computation time requirements, the mesh must be constructed using low-order elements that are computationally inexpensive. The linear under-integrated hexahedron is the preferred choice.

Many algorithms are now available for fast and accurate automatic mesh generation using tetrahedral elements, but not for automatic hexahedral mesh generation [20–22]. Template-based meshing algorithms can be used for discretising different organs using hexahedrons [23–25], but these types of algorithms only work for healthy organs. In the case of severe pathologies (such as a brain tumour or severely enlarged ventricles), such algorithms cannot be used as the shape, size and position of the pathology are unpredictable. This is one reason why many authors proposed the use of tetrahedral meshes for their models [5, 6, 26, 27]. In order to automate the simulation process, mixed meshes having both hexahedral and linear tetrahedral elements are the most convenient. Examples of such meshes are shown in Fig. 6.10 in the next section.

An alternative to using the finite element method is to use one of the available meshless methods. The problem of generating the computational grid disappears as one needs only to drop a cloud of points into the volume defined by a 3D medical image [1, 28–34]; see Fig. 6.5. Details of the meshless total Lagrangian explicit dynamics (MTLED) algorithm for computing soft tissue deformations are given in Chap. 11.

6.2.2 Boundary Conditions

The formulation of appropriate boundary conditions for computation of brain deformation during surgery constitutes a significant problem because of the complexity

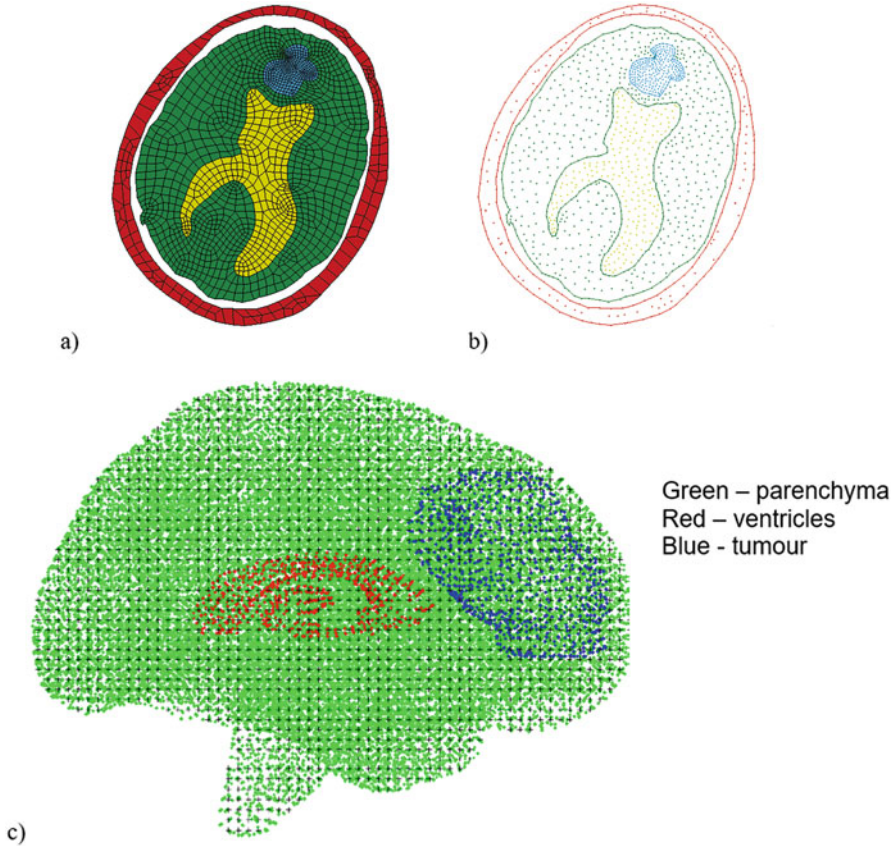


Fig. 6.5 A 2D slice of the brain discretised by (a) quadrilateral finite elements and (b) nodes of the modified element-free Galerkin method [35]. (c) 3D meshless discretisation of the brain [36]. Development of a good-quality finite element mesh is time-consuming; generation of the meshless grid is almost instantaneous

of the brain – skull interface (see Fig. 5.2 in Chap. 5 on modelling the brain for injury prevention where this problem is also highlighted).

A number of researchers ‘fix’ the brain surface to the skull [37, 38]. We do not recommend this approach as it is clearly inconsistent with the brain’s anatomy; see Chap. 2. One alternative is to use a gap between the brain and the skull that allows for motion of the brain within the cranial cavity [8, 39–44]. Another alternative is to use a frictionless sliding (with separation) contact model [45, 46] that can be incorporated into finite element computations very efficiently; see Chap. 10. This approach is partially supported by MR elastography measurements [47]. The reader should be aware that biomechanical knowledge about the properties of the brain-skull interface is very limited [48–51]. The brain-skull interface models used in the literature are ‘best guesses’ that, while effective in practice, might have little relation to reality.

The skull should be included in the model either explicitly or in the form of an appropriate boundary condition for the brain. As the skull is orders of magnitude stiffer than the brain tissue, it can be assumed to be rigid. The constraining effects of the spinal cord on the brain's rigid body motion can be simulated by constraining the spinal end of the model.

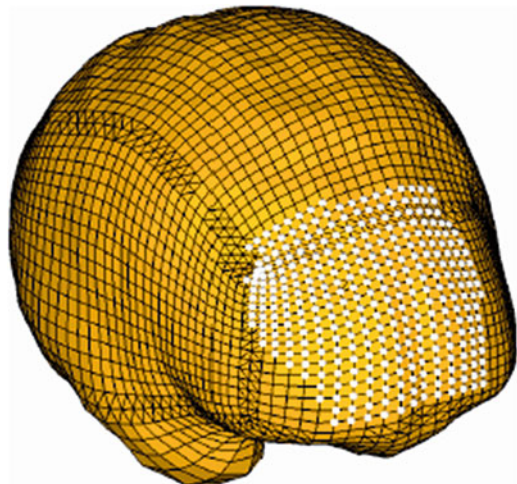
6.2.3 Loading

We advocate loading the models through imposed displacements on the model surface [41, 52]; see Fig. 6.6. In the case of neurosurgical simulation, this loading will be imposed by known motion of a surgical tool. In the case of intra-operative image registration, the current (intra-operative) position of the exposed part of the brain surface can be measured using various techniques; see Chaps. 12 and 13 of this book. This information can then be used to define model loading.

For problems where loading is prescribed as forced motion of boundaries, the unknown deformation field within the domain depends very weakly on the mechanical properties of the continuum [41, 52]. Because this feature is of great importance in biomechanical modelling, where there are always uncertainties in patient-specific properties of tissues, it warrants more detailed discussion.

If we consider an (oversimplified) quasistatic linear elastic case, the following dimensional reasoning applies. The loading is provided by the enforced motion of boundaries measured in metres [m]; the result of computations is displacements measured in [m]; therefore the result cannot depend on the stress parameter measured in [Pa = N/m²]. We should note here that the result can depend on (dimensionless) Poisson's ratio and on (dimensionless) ratios of stress parameters if the model contains materials with different stiffnesses. The dependence on

Fig. 6.6 Model loading through prescribed nodal displacements (on white surface nodes) at the exposed brain surface



the volumetric response (e.g. Poisson's ratio) is of minor consequence for soft organ biomechanics because tissues such as the brain, liver, kidney or prostate are considered almost incompressible; see, e.g. Chap. 4 of this book and [53–55].

In the general non-linear case, the displacement results will still remain insensitive to the stress parameter appearing in the non-linear material law but may depend on the particular form of that law (as the functional form of a constitutive law does not have a dimension). However, this dependency will be rather weak, as explicitly demonstrated in [56, 57] where the shapes of compressed and extended cylinders were shown to be essentially independent of the material law used for the cylinder's material; see Fig. 6.7. These results suggest a move away from mechanics towards kinematics where the main quantities of interest in this approach are displacements, strains and their histories.

We now consider nonrigid image registration in image-guided procedures where high-resolution pre-operative scans are warped onto lower-quality intra-operative images [58, 59]. The task of particular clinical interest is registering high-resolution pre-operative MRIs with lower-quality intra-operative imaging modalities, such as intra-operative ultrasound and multiplanar MRIs.

The brain, for which a detailed pre-operative image is available, deforms after craniotomy due to several physical and physiological reasons (i.e. brain shift, the specific mechanisms of the brain shift include decompression, response to anaesthesia and other possible and hotly contested phenomena). We are interested in the intra-operative (i.e. current) position of the brain, for which partial information is provided by low-resolution intra-operative images. In mathematical terms this problem can be described with equations of solid mechanics.

Consider the motion of a deforming body in a stationary coordinate system, Fig. 6.8. In the analysis we follow the motion of all particles from their original position to the final configuration of the body, which means that the Lagrangian (or material) formulation of the problem is adopted. Motion of the system sketched in Fig. 6.8 can be described by equations of motion often written in weak form:

$$\int_V \tau_{ij} \delta \varepsilon_{ij} dV = \int_V f_i^B \delta u_i dV + \int_S f_i^S \delta u_i dS \quad (6.1)$$

where ε is the Almansi strain, $\int_V \tau_{ij} \delta \varepsilon_{ij} dV$ is the internal virtual work, $\int_V f_i^B \delta u_i dV$ is the virtual work of external body forces (this includes inertial effects) and $\int_S f_i^S \delta u_i dS$ is the virtual work of external surface forces. As the brain undergoes finite deformation, the current volume V and surface S over which the integration is conducted are unknown: they are part of the solution rather than input data. Therefore, appropriate solution procedures which allow finite deformation must be used; see Chaps. 10 and 11. The integral Eq. (6.1) must be supplemented by formulae describing the mechanical properties of materials, i.e. appropriate constitutive models. However, an important advantage of the weak formulation is that the essential (displacement) boundary conditions are automatically satisfied [60].

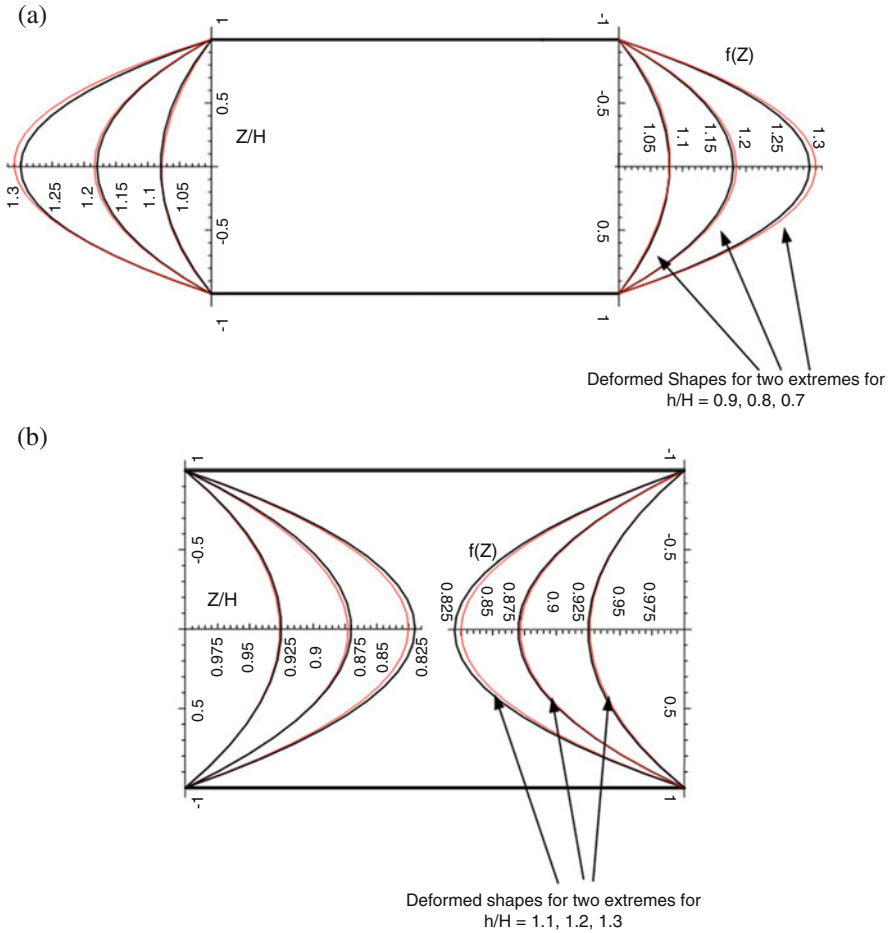
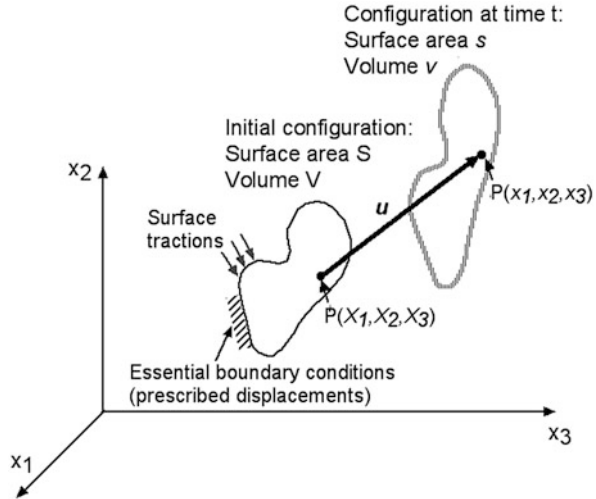


Fig. 6.7 Shapes of cylinders modelled as extreme-Mooney and neo-Hookean materials. **(a)** Compression by 10, 20 and 30%. **(b)** Extension by 10, 20 and 30%. Z/H denotes a dimensionless coordinate along the height of the cylinder. $f(Z)$ stands for the shape of the side of the deformed cylinder. The shape of a cylinder made from a ‘real’ material is expected to fall between the two extremes

Boundary conditions may prescribe kinematic variables such as displacements and velocities (essential boundary conditions) or tractions (natural boundary conditions, these also include concentrated forces). It should be noted that ‘boundary conditions’ do not have to be applied at the physical boundary of the deforming object: if convenient, they can be prescribed at, for example, the locations of easily identifiable anatomical landmarks with precisely known locations in both the pre-operative and intra-operative configuration of the brain.

Depending on the amount of information available about the intra-operative position of the brain from intra-operative imaging modalities, neuroimage registration

Fig. 6.8 Motion of a body in a stationary coordinate system. Initial configuration, described by uppercase coordinates, can be considered as a high-quality pre-operative image. Current, deformed configuration (described by lowercase coordinates) is unknown; however partial information is available from a lower-resolution intra-operative image



can be described mathematically in two ways. If the entire boundary of the brain can be extracted from the intra-operative image, then we know both the initial position of the domain (i.e. the brain), as determined from pre-operative MRI, and the current position of the entire boundary of the domain. We are looking for the unknown displacement field within the domain (the brain), in particular the current position of, for example, a tumour and healthy tissues (critically important from a surgical perspective). No information about surface tractions is required for the solution of this problem. In theoretical elasticity, problems of this type are called ‘pure displacement problems’ [61].

If only limited information is available about the boundary (e.g. only the position of the brain surface exposed during craniotomy and perhaps the current positions of clearly identifiable anatomical landmarks, as described in [62]) and no external forces are applied to the boundary, a slightly different mathematical description is needed. We know the initial position of the domain (i.e. the brain), as determined from pre-operative MRI, and the current position of some parts of the boundary of the domain (the brain), and we know that there are no pressure or traction forces everywhere else on the boundary. Consequently, contacts need to be modelled kinematically as in [45, 46]; see also Chap. 10 of this book. We do not know the displacement field within the domain (the brain), which means that we would not know the current positions of, for instance, a tumour and healthy tissues.

Problems of this type are very special cases of ‘displacement – traction problems’ [61] that have not, to the best of our knowledge, been considered as a separate class, and no special methods of solution for these problems exist. Reference [63] contains the suggestion to call such problems ‘displacement – zero traction problems’. More recently we named such problems Dirichlet-type [52].

The solutions in displacements (the variable of interest in the context of image-guided surgery) for both pure displacement and displacement-zero traction

Table 6.1 Comparison of predicted displacements of tumour and ventricle centres of gravity obtained with various constitutive models [41]. It is clear that while using the proper non-linear solution procedure is essential, the choice of constitutive model makes little difference

Center of Gravity Displacements (mm)						
Material Model/ Analysis Type	Ventricles			Tumor		
	ΔX	ΔY	ΔZ	ΔX	ΔY	ΔZ
MRI Determined	3.4	0.2	1.7	5.5	-0.2	1.7
Hyperviscoelastic material/ Geometrically non-linear analysis	2.6	-0.1	2.1	5.2	-0.4	2.7
Hyperelastic material/ Geometrically non-linear analysis	2.6	-0.1	2.1	5.2	-0.4	2.7
Linear elastic material/ Geometrically non-linear analysis	2.6	-0.1	2.1	5.0	-0.5	2.7
Linear elastic material/ Linear analysis	0.7	0.2	1.9	3.7	-0.3	2.6

problems (Dirichlet-type) are only very weakly sensitive to mechanical properties of the deforming continuum and therefore can be obtained without knowledge of patient-specific properties of the brain tissue.

In the case of the full-scale brain deformation computation, our experience confirms the expected insensitivity of computed displacement fields to different tissue constitutive models [41]. Table 6.1 contains observed and computed displacements for centres of gravity of ventricles and tumour for a case of tumour removal described in detail in [41]. In the computations the same general geometrically non-linear formulation was used together with various constitutive models.

When interpreting the results summarised in Table 6.1, note that the accuracy of determining positions of centres of gravity of tumour and ventricles is limited by the voxel size in the intra-operative MRI images used in this study – 0.85 mm \times 0.85 mm \times 2.5 mm. We also need to consider that the accuracy of manual neurosurgery is approximately 1 mm [7]. Therefore, for practical purposes, values differing by less than 0.80 mm can be considered equivalent. The slightly different results seen in the second-last row of Table 6.1 are due to the fact that the linear elastic constitutive model is not compatible with the finite deformation solution procedure [64]. It is apparent that the choice of the constitutive model does not make any practical difference in the solution for displacements, and therefore we recommend the use of neo-Hookean material model. However, if geometrically linear analysis is used – see the last row of Table 6.1 – the results are clearly erroneous.

6.2.4 *Models of Mechanical Properties of Brain Tissue*

The first question to address is whether a single-phase continuum model for the tissue should be used or if biphasic or even more complicated multiphase models are required. Many researchers conclude that the brain is obviously a hydrated tissue and therefore use biphasic models based on consolidation theory; see, e.g. [65] and references cited therein. We are of the opinion that biphasic, consolidation theory-based models are inconsistent with brain tissue behaviour observed in simple experiments. For example, no leakage of CSF was observed in brain tissue samples loaded by CSF pressure difference [66, 67]. Another argument against using biphasic models is that during numerous unconfined compression experiments [68], we never observed fluid leaking from the side of the samples. Such leakage is predicted by biphasic theory. Therefore, in the remainder of this chapter, we will discuss only single-phase modelling approaches.

Experimental results show that the mechanical response of brain tissue to external loading is very complex. The stress-strain relationship is clearly non-linear with no portion in the plots suitable for estimating a meaningful Young's modulus. It is also obvious that the stiffness of the brain in compression is much higher than in extension [69]. The non-linear relationship between stress and strain rate is also apparent. Detailed exposition of the current knowledge about the mechanical properties of brain tissue is given in Chap. 4. Here we will only discuss issues directly pertinent to modelling neurosurgery.

The great majority of brain models assume brain tissue is *incompressible* and *isotropic* (see also Chaps. 4 and 5). The assumption of incompressibility is not contentious. Whether it is reasonable to assume that brain tissue is isotropic (i.e. mechanical properties the same in all directions) is less clear, especially in view of the obviously directional character of white matter fibres. Brain tissues do not normally bear mechanical loads and do not exhibit directional structure, provided that a large-enough length scale is considered. Therefore, they may be assumed to be initially isotropic; see, e.g. [69–77]. When modelling brain deformations during surgery, we need to keep in mind that the accuracy of displacement computations rarely needs to be better than about 1 mm – the claimed accuracy of neurosurgery. Therefore, ‘average isotropic’ properties at the length scales relevant to surgical procedures are most probably sufficient. These properties are relatively well accounted for by an Ogden-type hyperviscoelastic model [78] described in Chap. 4, Eqs. 4.4 and 4.5.

Average properties, such as those described above, are not sufficient for patient-specific computations of stresses and reaction forces because of the very large variability inherent in biological materials. This variability is clearly demonstrated in the biomechanics literature [69, 80–81]. Unfortunately, despite recent progress in elastography using ultrasound [82, 83] and magnetic resonance (see Chap. 4) [84–88], reliable methods of measuring patient-specific properties of the brain are not yet available.

Nevertheless, as shown in the previous section on modelling loading, much can be achieved even without a patient-specific model of brain tissue mechanical properties, if the model is loaded by the enforced motion of a boundary and the problem is formulated as Dirichlet-type: a pure displacement or displacement-zero traction problem. As the computed results are then almost insensitive to the assumed mechanical properties of the tissue, we advocate using the simplest model that is compatible with finite deformation solution procedures, a neo-Hookean model:

$${}^t_0S = \mu \cdot J^{-2/3} \left(I_3 - \frac{1}{3} \cdot I_0^t C^{-1} \right) + k \cdot (J - 1) \cdot J \cdot {}^t_0C^{-1} \quad (6.2)$$

where t_0S is the second Piola-Kirchhoff stress, I is the first invariant of the deviatoric right Cauchy-Green deformation tensor C (the first strain invariant), J is the determinant of the deformation gradient (representing the volume change), I_3 is the 3×3 identity matrix, μ is the shear modulus and k is the bulk modulus of the material.

The accuracy of this approach is demonstrated in Sect. 6.3 of this chapter.

6.2.5 Model Validation

For mathematical modelling and computer simulation to be of any practical use – to be *reliable* [89] – the results derived from the models must be known to lie within the prescribed margins of accuracy. As we have seen in Chap. 5, ascertaining that this is the case when modelling high-speed impacts and brain injury is a very difficult task. Modellers of the brain for neurosurgery are however in a better position: they have at their disposal intra-operative imaging modalities (see Chap. 12) providing images that can be used for a relatively straightforward validation of the results of computer simulations of brain deformations.

Biomechanical models of the brain contain a lot of simplifying assumptions to make them mathematically and computationally tractable. To be of practical use, solutions to these models must be obtained in real or close to real time. Therefore nonstandard specially designed solution algorithms and software implementations are often used (see Chaps. 10 and 11). It is very important, and unfortunately overlooked by many researchers, that the biomechanical model and solution method be validated separately. If we were to evaluate a ‘software system’ consisting of implemented nonstandard solution algorithms to a complicated biomechanical model and found discrepancies when compared with experiments, we would have no indication whether these discrepancies arose from inappropriate modelling assumptions or faulty numerical procedure (or both).

We recommend that new real-time solution algorithms be verified against well-established solution procedures implemented in commercial software. The assumptions of the biomechanical model need to be evaluated against available experimental data. The biomechanical model should then be validated by comparing the solutions computed using established numerical procedures and experimental results. If these hurdles are cleared and it can be also demonstrated that replacing established numerical procedures with the specialised ones developed for real-time applications does not affect the computed results, then one may treat the ‘software system’ with some degree of confidence.

How accurate should the results of the computational biomechanics model of the brain be? Accuracy of manual neurosurgery is not better than 1 mm. The voxel size of the best available experimental tool for model validation – currently the intra-operative MRI – is of the same order. Therefore, the computed intra-operative displacements do not need to be more accurate than about 1 mm. We may note here that, paradoxically, this accuracy requirement is much less stringent than those used in traditional engineering disciplines. In image-guided surgery applications, we are not interested in stress distributions, only in the displacement field. This is one of the reasons why simple constitutive models of the brain tissue can be used. However, for surgical simulation applications, we need to compute reaction forces on surgical tools that will be fed back to the user through a haptic interface. At present there is no consensus regarding how accurate this haptic feedback should be to facilitate a realistic experience. Given the present state of biomechanical knowledge, the best that can be achieved is qualitative agreement between real and computed interaction forces; see, e.g. [71]. This is despite examples of excellent agreement between computations and phantom experiments [90] as well as controlled in vitro experiments [91].

6.3 Application Example: Computer Simulation of Brain Shift

A particularly exciting application of nonrigid image registration is in intra-operative image-guided procedures, where pre-operative scans are warped onto sparse intra-operative images [7, 58]. We are especially interested in registering high-resolution pre-operative MRIs with lower-quality intra-operative imaging modalities, such as multiplanar MRIs and intra-operative ultrasound. To achieve accurate matching of these modalities, precise and fast algorithms to compute tissue deformations are fundamental.

Here we present selected results of the analysis of 33 cases of craniotomy-induced brain shift representing different situations that may occur during neurosurgery [92, 93].

6.3.1 *Generation of Computational Grids: From Medical Images to Finite Element Meshes*

Pre-operative and intra-operative medical image datasets of 33 patients with cerebral gliomas were randomly selected from a retrospective database of 859 intracranial tumour cases available at Boston Children's Hospital [94]. Imaging was performed using a 0.5 T open MR system in the neurosurgical suite. The resolution of the images is $0.85 \times 0.85 \times 2.5 \text{ mm}^3$. Consent was obtained for the use of the anonymised retrospective image database, in accordance with the Institutional Review Board of Boston Children's Hospital.

A three-dimensional (3D) surface model of each patient's brain was created from segmented pre-operative magnetic resonance images (MRIs). Following our previous studies on predicting craniotomy-induced deformations within the brain [11, 95–98], in this investigation, different material properties were assigned to the parenchyma, tumour and ventricles. Accordingly, to obtain the information for building the computational grids (finite element meshes), the parenchyma, tumour and ventricles were segmented using the region growing algorithm implemented in 3D Slicer, followed by manual correction.

The meshes were constructed using low-order elements (linear tetrahedron or hexahedron) to meet the requirement that computations be conducted intra-operatively, i.e. within no more than ca. 1 min. To prevent volumetric locking, tetrahedral elements with average nodal pressure (ANP) formulation were used [99]. The meshes were generated using IA-FEMesh [100] and HyperMesh (commercial FE mesh generator by Altair of Troy, MI, USA). A typical mesh (Case 1) is shown in Fig. 6.9. This mesh consists of 14,447 hexahedral elements, 13,563 tetrahedral elements and 18,806 nodes. Each node in the mesh has three degrees of freedom.

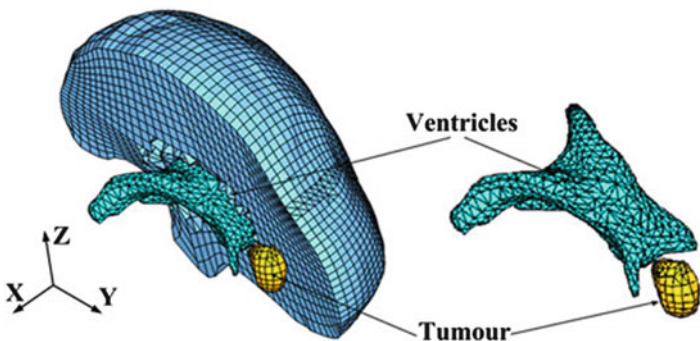


Fig. 6.9 Typical example (Case 1) of a patient-specific mesh built for this study. This mesh consists of 14,447 hexahedral elements, 13,563 tetrahedral elements and 18,806 nodes

6.3.2 Displacement Loading

The models were loaded by prescribing displacements on the exposed part (due to craniotomy) of the brain surface. As this requires only replacing the brain-skull contact boundary condition with prescribed displacements, no mesh modification is required at this stage. At first the pre-operative and intra-operative coordinate systems were aligned by rigid registration. Then the displacements at the mesh nodes located in the craniotomy region were estimated with the interpolation algorithm we described in [101].

As explained above (Sect. 2.3 and 2.4), for problems where loading is prescribed as forced motion of boundaries, the unknown deformation field within the domain depends very weakly on the mechanical properties of the continuum. This feature is of great advantage in biomechanical modelling where there are always uncertainties in patient-specific properties of tissues [102].

6.3.3 Boundary Conditions

The stiffness of the skull is several orders of magnitude higher than that of the brain tissue. Therefore, in order to define the boundary conditions for the unexposed nodes of the brain mesh, a contact interface [103] was defined between the rigid skull model and the deformable brain. The interaction was formulated as a finite sliding, frictionless contact between the brain and the skull. The effects of assumptions regarding the brain boundary conditions on the results of prediction of deformations within the brain have been analysed and discussed in [96, 104] and more recently in [51].

6.3.4 Mechanical Properties of the Intracranial Constituents

For Dirichlet-type problems, the predicted deformation field within the brain is only weakly affected by the constitutive model of the brain tissue [98]. Therefore, for simplicity a hyper-elastic neo-Hookean model was used [105]. The Young's modulus of 3000 Pa was selected for parenchyma [106]. The Young's modulus for tumour was assigned a value two times larger than that for the parenchyma, keeping it consistent with the experimental data of Sinkus et al. [107]. As the brain tissue is almost incompressible, a Poisson's ratio of 0.49 was chosen for the parenchyma and tumour [96]. The ventricles were assigned properties of a very soft compressible elastic solid with a Young's modulus of 10 Pa and Poisson's ratio of 0.1 [96].

6.3.5 *Solution Algorithm*

A suite of efficient algorithms for integrating the equations of solid mechanics and its implementation on a graphics processing unit for real-time applications are described in detail in Chap. 10 and [11, 108]. The computational efficiency of this algorithm is achieved by using a total Lagrangian (TL) formulation [109] for updating the calculated variables and an explicit integration in the time domain combined with mass proportional damping. In the TL formulation, all the calculated variables (such as displacements and strains) are referred to the original configuration of the analysed continuum [111]. The decisive advantage of this formulation is that all derivatives with respect to spatial coordinates can be precomputed. The total Lagrangian formulation also leads to a simplification of the material law implementation as these material models can be easily described using the deformation gradient [108].

The integration of equilibrium equations in the time domain was performed using an explicit method. When a diagonal (lumped) mass matrix is used, the discretised equations are decoupled. Therefore, no matrix inversions and iterations are required when solving non-linear problems. Application of the explicit time integration scheme reduces the time required to compute the brain deformations by two orders of magnitude in comparison to implicit integration typically used in commercial finite element codes like ABAQUS [112]. This algorithm is also implemented on GPU (NVIDIA Tesla C1060 installed on a PC with Intel Core2 Quad CPU) for real-time computation [11] so that the entire model solution takes less than 4 seconds on commonly available hardware.

The application of the biomechanics-based approach does not require any parameter tuning, and the results presented in the next section demonstrate the predictive (rather than explanatory) power of this method.

6.3.6 *Results and Validation*

6.3.6.1 *Qualitative Evaluation*

Deformation field The physical plausibility of the registration results is verified by examining the computed displacement vector at voxels of the pre-operative image domain. The deformations are computed at voxel centres only for a region of interest near the tumour.

Overlap of edges To obtain a qualitative assessment of the degree of alignment after registration, one must examine the overlap of corresponding anatomical features of the intra-operative and registered pre-operative image. For this purpose, tumours and ventricles in both registered pre-operative and intra-operative images can be segmented, and their surfaces can be compared [97]. Image segmentation is time-consuming, subjective, not fully automated and not suitable for comparing

a large number of image pairs [113]. Therefore we chose Canny edges [114] as features for comparison [9]. Edges are regarded as useful and easily recognisable features, and they can be detected using techniques that are automated and fast. Canny edges obtained from the intra-operative and registered pre-operative image slices are labelled in different colours and overlaid.

6.3.6.2 Quantitative Evaluation

For a quantitative evaluation of the accuracy of the displacement calculations, we used the edge-based Hausdorff distance. This methodology, based on pioneering work of [115], is described in detail in [9].

While measuring the misalignments between two medical images, it is desirable to calculate the distance between local features (in the case of brain MRI considered here, the automatically detected Canny edges) in two images that correspond to each other. We define directed distance between two sets of edges as

$$h_e(\mathbf{A}^e, \mathbf{B}^e) = \arg \max_{a_i^e \in \mathbf{A}^e} \left[\arg \min_{b_j^e \in \mathbf{B}^e} \|a_i^e - b_j^e\| \right] \quad (6.3)$$

where $\mathbf{A}^e = \{a_1^e, \dots, a_m^e\}$ and $\mathbf{B}^e = \{b_1^e, \dots, b_n^e\}$ are two sets of edges.

The quantity $\|a_i^e - b_j^e\|$ in Eq. 6.3 is just the point-based Hausdorff distance between two point sets $\mathbf{M} = \{m_1, \dots, m_p\}$ and $\mathbf{T} = \{t_1, \dots, t_q\}$ representing edges a_i^e and b_j^e , respectively,

$$\|a_i^e - b_j^e\| := d(a_i^e - b_j^e) = \max(h(\mathbf{T}, \mathbf{M}), h(\mathbf{M}, \mathbf{T})) \quad (6.4)$$

Now the edge-based Hausdorff distance is defined as

$$H_e(\mathbf{A}^e, \mathbf{B}^e) = \max(h_e(\mathbf{A}^e, \mathbf{B}^e), h_e(\mathbf{B}^e, \mathbf{A}^e)) \quad (6.5)$$

Similar to the percentile point-based Hausdorff distance, one can construct a percentile edge-based Hausdorff distance:

$$h_{P_e}(\mathbf{A}^e, \mathbf{B}^e) = \underset{a_i^e \in \mathbf{A}^e}{P^{\text{th}}} \left[\arg \min_{b_j^e \in \mathbf{B}^e} \|a_i^e - b_j^e\| \right] \quad (6.6)$$

This percentile edge-based Hausdorff distance is not only useful for removing outlier edge pairs but can also be interpreted in a different way. The Pth percentile Hausdorff distance, ‘D’, between two images means that ‘P’ percent of total edge pairs has a Hausdorff distance below D. Therefore, instead of reporting only one Hausdorff distance value (using Eq. 6.5), Eq. 6.6 can be used to report Hausdorff

distance values for different percentiles. A plot of the Hausdorff distance values at different percentiles immediately reveals the percentage of edges that have misalignments below an acceptable error.

6.3.6.3 Results

Qualitative Evaluation of Registration Results

Deformation Field

The deformation fields predicted by the biomechanical model are compared to these obtained from the BSpline transform (available in 3D Slicer [116]) used to register pre- to intra-operative neuroimages. These deformation fields are three dimensional. However, for clarity, only arrows representing 2D vectors (x and y components of displacement) are shown overlaid on undeformed pre-operative slices. Each of these arrows represents the displacement of a voxel of the pre-operative image domain. In general the displacement fields calculated by the BSpline registration algorithm are similar to the predicted displacements by the biomechanical model at the outer surface of the brain, but in the interior of the brain volume, the displacement vectors differ in both magnitude and direction (Fig. 6.10).

Overlap of Canny Edges

From Fig. 6.11 we can see that misalignment between the edges detected from the intra-operative images and the edges from the pre-operative images updated to the intra-operative brain geometry is much lower for the biomechanics-based warping than for BSpline registration. This is an indication that the biomechanics-based prediction of brain deformations may perform more reliably than the BSpline registration algorithm if large deformations are involved.

Quantitative Evaluation of Registration Results

The plot of percentile edge-based Hausdorff distance (HD) versus the corresponding percentile provides an estimation of the percentage of edges whose displacements have been computed with sufficient accuracy. As the accuracy of edge detection is limited by the image resolution, an alignment error smaller than two times the original in-plane resolution of the intra-operative image (which is 0.86 mm for the 13 cases considered) is difficult to avoid [117]. Hence, for the clinical cases analysed here, we considered any edge pair having an HD value less than 1.7 mm to be successfully registered. This choice is consistent with the fact that it is generally considered that manual neurosurgery has an accuracy of no better than 1 mm [117, 118]. It is obvious from Fig. 6.12 that biomechanical warping was able to successfully register more edges than the BSpline registration.

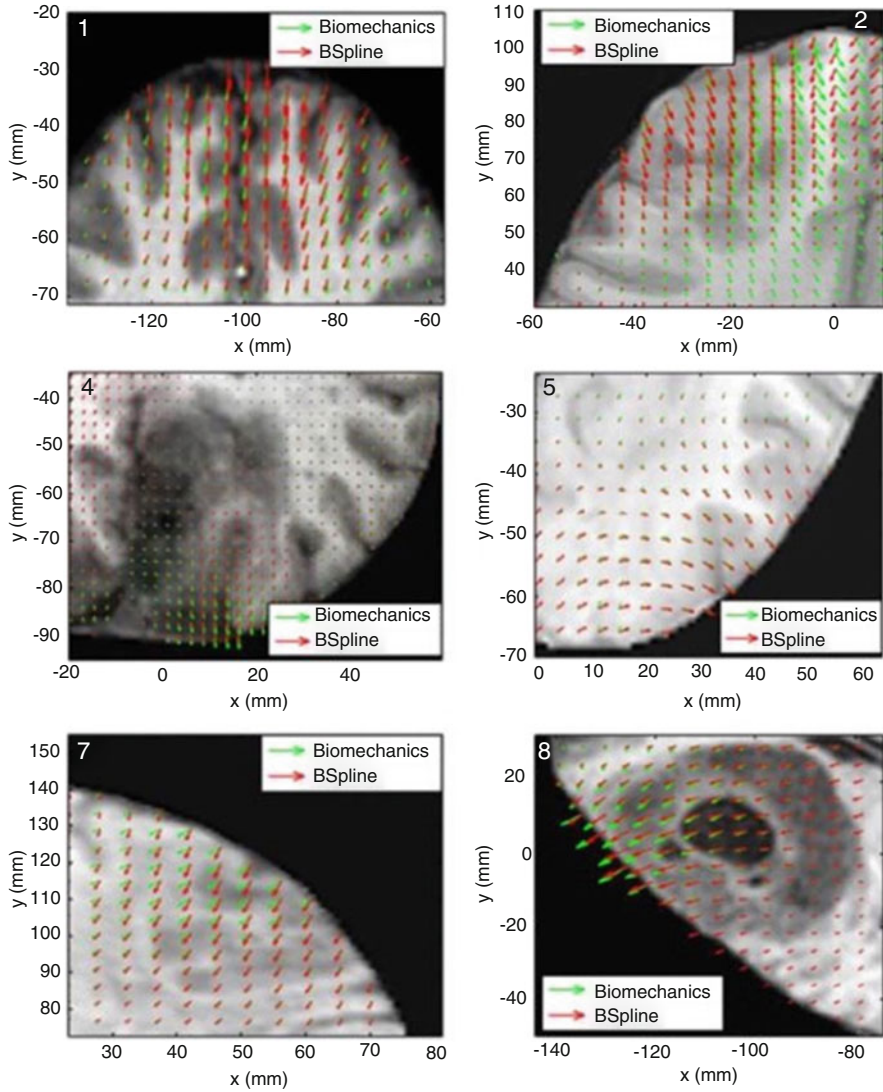


Fig. 6.10 The predicted deformation fields overlaid on an axial slice of pre-operative image (six examples). An arrow represents a 2D vector consisting of the x (R-L) and y (A-P) components of displacement at a voxel centre. Green arrows show the deformation field predicted by the biomechanical model. Red arrows show the deformation field calculated by the BSpline algorithm. The number on each image denotes a particular neurosurgery case. (Modified from [93])

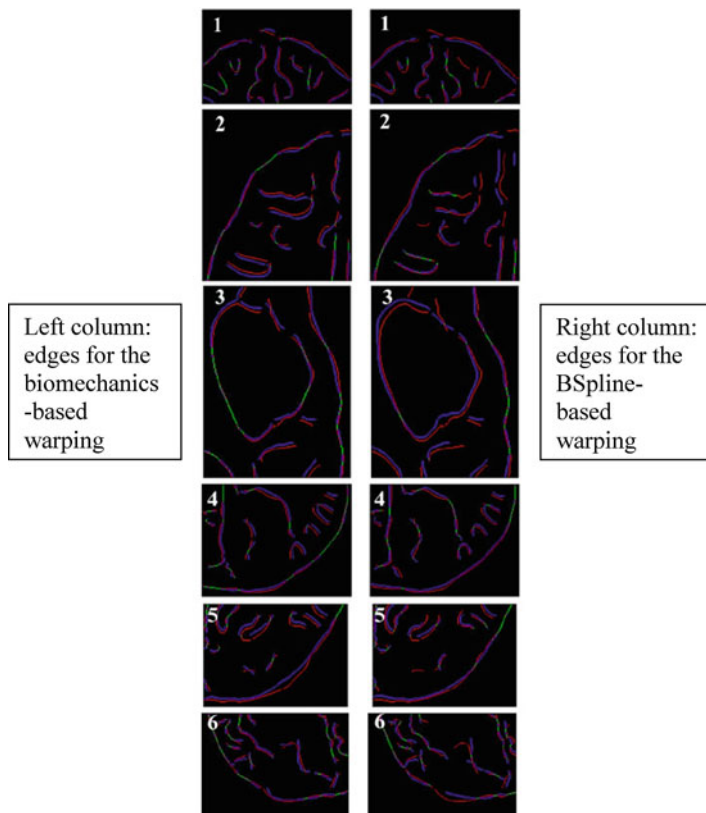


Fig. 6.11 Canny edges extracted from intra-operative and the registered pre-operative image slices overlaid on each other. Red lines represent the nonoverlapping pixels of the intra-operative slice, and blue lines represent the nonoverlapping pixels of the pre-operative slice. Green lines represent the overlapping pixels. The number on each image denotes a particular neurosurgery case. For each case, the left image shows edges for the biomechanics-based warping, and the right image shows edges for the BSpline-based registration. (Image modified from [81])

6.4 Conclusions

Computational mechanics has become a central enabling discipline that has led to greater understanding and advances in modern science, technology and engineering [119]. It is now in a position to make a similar impact in medicine. We have discussed modelling approaches to two applications of clinical relevance: surgical simulation and neuroimage registration. These problems can be reasonably characterised with the use of purely mechanical terms such as displacements, internal forces, etc. Therefore they can be analysed using the methods of continuum mechanics. Moreover similar methods may find applications in modelling the development of structural diseases of the brain [42, 120–122].

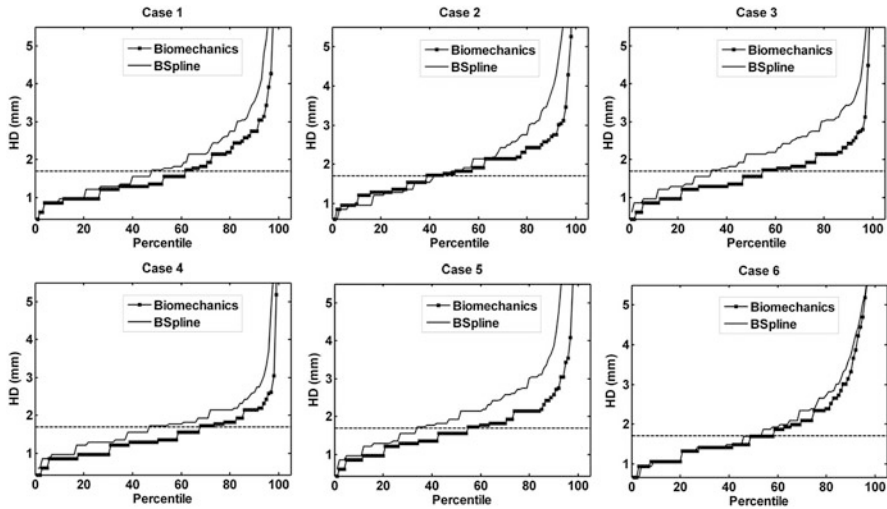


Fig. 6.12 The plot of percentile edge-based Hausdorff distance between intra-operative and registered pre-operative images against the corresponding percentile of edges for axial slices. The horizontal line is the 1.7 mm mark. Six representative examples. Image modified from [93]

As the brain undergoes large displacements ($\sim 10\text{--}20$ mm in the case of a brain shift) and its mechanical response to external loading is strongly non-linear, we advocate the use of general, non-linear procedures for the numerical solution of the proposed models.

The brain's complicated mechanical behaviour: non-linear stress-strain, stress-strain-rate relationships and much lower stiffness in extension than in compression require very careful selection of the constitutive model for a given application. The selection of the constitutive model for surgical simulation problems depends on the characteristic strain rate of the process to be modelled and to a certain extent on computational efficiency considerations. Fortunately, as shown in Sections 6.2.3 and 6.2.4, as well as in [41, 52], the precise knowledge of patient-specific mechanical properties of brain tissue is not required for intra-operative image registration.

A number of challenges must be met before computer-integrated surgery systems based on computational biomechanical models can become as widely used as computer-integrated manufacturing systems are now. As we deal with individual patients, methods to produce patient-specific computational grids quickly and reliably must be improved [1]. Substantial progress in automatic meshing methods is required, or alternatively meshless methods [12] may provide a solution (see Chap. 12 of this book). Computational efficiency is an important issue, as intra-operative applications, requiring reliable results within approximately 40 seconds, are most appealing. Progress can be made in non-linear algorithms by identifying parts that can be precomputed and parts that do not have to be calculated at every time step. One such possibility is to use the total Lagrangian formulation of the finite element method [64, 109, 123], where all field variables are related to the original (known) configuration of the system, and therefore most spatial derivatives

can be calculated before the simulation commences during the preprocessing stage (see Chap. 10 of this book). Implementation of algorithms in parallel on networks of processors and harnessing the computational power of graphics processing units [11] provide a challenge for the coming years.

Acknowledgements The financial support of the Australian Research Council (Grants No. DP0343112, DP0664534, DP1092893, DP120100402, DP160100714 and LX0560460), National Health and Medical Research Council (Australia) (APP1006031, APP1144519, APP1162030) and National Institutes of Health (Grant No. 1-RO3-CA126466-01A1) is gratefully acknowledged. We thank our collaborators Dr. Ron Kikinis and Dr. Simon Warfield from Harvard Medical School and Dr. Kiyoyuki Chinzei and Dr. Toshikatsu Washio from Surgical Assist Technology Group of AIST, Japan, for the help in various aspects of our work.

The medical images used in the present study (provided by Dr. Simon Warfield) were obtained in the investigation supported by a research grant from the Whitaker Foundation and by NIH grants R21 MH67054, R01 LM007861, P41 RR13218 and P01 CA67165.

We thank Toyota Central R&D Labs. (Nagakute, Aichi, Japan) for providing the THUMS brain model.

References

1. Wittek, A., Grosland, N.M., Joldes, G.R., Magnotta, V., Miller, K.: From finite element meshes to clouds of points: a review of methods for generation of computational biomechanics models for patient-specific applications. *Ann. Biomed. Eng.* **44**(1), 3–15 (2016)
2. Bucholz, R., MacNeil, W., McDurmont, L.: The operating room of the future. *Clin. Neurosurg.* **51**, 228–237 (2004)
3. Nakaji, P., Speltzer, R.F.: Innovations in surgical approach: the marriage of technique, technology, and judgement. *Clin. Neurosurg.* **51**, 177–185 (2004)
4. Roberts, D.W., Hartov, A., Kennedy, F.E., Miga, M.I., Paulsen, K.D.: Intraoperative brain shift and deformation: a quantitative analysis of cortical displacement in 28 cases. *Neurosurgery.* **43**, 749–758 (1998)
5. Ferrant, M., Nabavi, A., Macq, B., Black, P., Jolesz, F.A., Kikinis, R., Warfield, S.K.: Serial registration of interoperative MR images of the brain. *Med. Image Anal.* **6**(4), 337–359 (2002)
6. Warfield, S.K., Talos, F., Tei, A., Bharatha, A., Nabavi, A., Ferrant, M., Black, P.M., Jolesz, F.A., Kikinis, R.: Real-time registration of volumetric brain MRI by biomechanical simulation of deformation during image guided neurosurgery. *Comput. Vis. Sci.* **5**, 3–11 (2002)
7. Warfield, S.K., Haker, S.J., Talos, F., Kemper, C.A., Weisenfeld, N., Mewes, A.U.J., Goldberg-Zimring, D., Zou, K.H., Westin, C.F., Wells III, W.M., Tempany, C.M.C., Golby, A., Black, P.M., Jolesz, F.A., Kikinis, R.: Capturing intraoperative deformations: research experience at Brigham and Women’s hospital. *Med. Image Anal.* **9**(2), 145–162 (2005)
8. Wittek, A., Miller, K., Kikinis, R., Warfield, S.K.: Patient-specific model of brain deformation: application to medical image registration. *J. Biomech.* **40**, 919–929 (2007)
9. Garlapati, R.R., Mostayed, A., Joldes, G.R., Wittek, A., Doyle, B., Miller, K.: Towards measuring neuroimage misalignment. *Comput. Biol. Med.* **64**, 12–23 (2015)
10. Mostayed, A., Garlapati, R.R., Joldes, G.R., Wittek, A., Roy, A., Kikinis, R., Warfield, S.K., Miller, K.: Biomechanical model as a registration tool for image-guided neurosurgery: evaluation against BSpline registration. *Ann. Biomed. Eng.* **41**(11), 2409–2425 (2013)
11. Joldes, G.R., Wittek, A., Miller, K.: Real-time nonlinear finite element computations on GPU - application to neurosurgical simulation. *Comput. Methods Appl. Mech. Eng.* **199**(49–52), 3305–3314 (2010)

12. Joldes, G.R., Bourantas, G., Zwick, B., Chowdhury, H., Wittek, A., Agrawal, S., Mountris, K., Hyde, D., Warfield, S.K., Miller, K.: Suite of meshless algorithms for accurate computation of soft tissue deformation for surgical simulation. *Med. Image Anal.* **56**, 152–171 (2019)
13. Halle, M., Talos, I-F., Jakab, M., Makris, N., Meier, D., Wald, L., Fischl, B., Kikinis, R.: Multi-modality MRI-based Atlas of the Brain. 2017 [cited 2018; Available from: <http://www.spl.harvard.edu/publications/item/view/2037>
14. Arani, A., Murphy, M.C., Glaser, K.J., Manduca, A., Lake, D.S., Kruse, S.A., Jack Jr., C.R., Ehman, R.L., Huston 3rd, J.: Measuring the effects of aging and sex on regional brain stiffness with MR elastography in healthy older adults. *NeuroImage*. **111**, 59–64 (2015)
15. Guo, J., Hirsch, S., Fehlner, A., Papazoglou, S., Scheel, M., Braun, J., Sack, I.: Towards an elastographic atlas of brain anatomy. *PLoS One*. **8**(8), e71807 (2013)
16. Hughes, J.D., Fattahi, N., Van Gompel, J., Arani, A., Meyer, F., Lanzino, G., Link, M.J., Ehman, R., Huston, J.: Higher-resolution magnetic resonance elastography in meningiomas to determine intratumoral consistency. *Neurosurgery*. **77**(4), 653–658; discussion 658–9 (2015)
17. Reiss-Zimmermann, M., Streitberger, K.J., Sack, I., Braun, J., Arlt, F., Fritzsche, D., Hoffmann, K.T.: High resolution imaging of viscoelastic properties of intracranial tumours by multi-frequency magnetic resonance elastography. *Clin. Neuroradiol.* **25**(4), 371–378 (2015)
18. Murphy, M.C., Huston 3rd, J., Glaser, K.J., Manduca, A., Meyer, F.B., Lanzino, G., Morris, J.M., Felmlee, J.P., Ehman, R.L.: Preoperative assessment of meningioma stiffness using magnetic resonance elastography. *J. Neurosurg.* **118**(3), 643–648 (2013)
19. Garlapati, R.R., Roy, A., Joldes, G.R., Wittek, A., Mostayed, A., Doyle, B., Warfield, S.K., Kikinis, R., Knuckey, N., Bunt, S., Miller, K.: Biomechanical modeling provides more accurate data for neuronavigation than rigid registration. *J. Neurosurg.* **120**(6), 1477–1483 (2014)
20. Owen, S.J.: A survey of unstructured mesh generation technology. In: 7th International Meshing Roundtable. Dearborn, Michigan, USA, (1998)
21. Viceconti, M., Taddei, F.: Automatic generation of finite element meshes from computed tomography data. *Crit. Rev. Biomed. Eng.* **31**(1), 27–72 (2003)
22. Owen, S.J.: Hex-dominant mesh generation using 3D constrained triangulation. *Comput. Aided Des.* **33**, 211–220 (2001)
23. Castellano-Smith, A.D., et al.: Constructing patient specific models for correcting intraoperative brain deformation. In: 4th International Conference on Medical Image Computing and Computer Assisted Intervention MICCAI Lecture Notes in Computer Science 2208. Utrecht, The Netherlands (2001)
24. Couteau, B., Payan, Y., Lavallée, S.: The mesh-matching algorithm: an automatic 3D mesh generator for finite element structures. *J. Biomech.* **33**, 1005–1009 (2000)
25. Luboz, V., Chabanas, M., Swider, P., Payan, Y.: Orbital and maxillofacial computer aided surgery: patient-specific finite element models to predict surgical outcomes. *Comput. Methods Biomech. Biomed. Eng.* **8**(4), 259–265 (2005)
26. Ferrant, M., Macq, B., Nabavi, A., Warfield, S.K.: Deformable modeling for characterizing biomedical shape changes. In: Discrete Geometry for Computer Imagery: 9th International Conference. Springer, Uppsala (2000)
27. Clatz, O., Delingette, H., Bardinet, E., Dormont, D., Ayache, N.: Patient specific biomechanical model of the brain: application to Parkinson’s disease procedure. In: International Symposium on Surgery Simulation and Soft Tissue Modeling (IS4TM’03), Springer, Juan-les-Pins (2003)
28. Horton, A., Wittek, A., Miller, K.: Computer simulation of brain shift using an element free Galerkin method. In: 7th International Symposium on Computer Methods in Biomechanics and Biomedical Engineering CMBEE 2006. Antibes, France (2006)
29. Horton, A., Wittek, A., Miller, K.: Towards meshless methods for surgical simulation. In: Computational Biomechanics for Medicine Workshop, Medical Image Computing and Computer-Assisted Intervention MICCAI 2006. Copenhagen, Denmark (2006)
30. Horton, A., Wittek, A., Miller, K.: Subject-specific biomechanical simulation of brain indentation using a meshless method. In: International Conference on Medical Image Computing and Computer-Assisted Intervention MICCAI 2007. Springer, Brisbane (2007)

31. Belytschko, T., Lu, Y.Y., Gu, L.: Element-free Galerkin methods. *Int. J. Numer. Methods Eng.* **37**, 229–256 (1994)
32. Liu, G.R.: *Mesh Free Methods: Moving Beyond the Finite Element Method*. CRC Press, Boca Raton (2003)
33. Li, S., Liu, W.K.: *Meshfree Particle Methods*. Springer-Verlag Berlin Heidelberg (2004)
34. Horton, A., Wittek, A., Joldes, G., Miller, K.: A meshless Total Lagrangian explicit dynamics algorithm for surgical simulation. *Int. J. Numer. Methods Biomed. Eng.* **26**, 117–138 (2010)
35. Zhang, J.Y., Joldes, G.R., Wittek, A., Horton, A., Warfield, S.K., Miller, K.: Neuroimage as a biomechanical model. Towards new computational biomechanics of the brain. In: Nielsen, P.M.F., Miller, K., Wittek, A. (eds.) *Computational Biomechanics for Medicine: Deformation and Flow*, pp. 19–28. Springer, New York (2012)
36. Miller, K., Horton, A., Joldes, G., Wittek, A.: Beyond finite elements: a comprehensive, patient-specific neurosurgical simulation utilising a meshless method. *J. Biomech.* (2012). Accepted for publication on 31 July 2012
37. Hagemann, A., Rohr, K., Stiehl, H.S., Spetzger, U., Gilsbach, J.M.: Biomechanical modeling of the human head for physically based, nonrigid image registration. *IEEE Trans. Med. Imaging – Special Issue Model-Based Anal Med Images.* **18**(10), 875–884 (1999)
38. Miga, M.I., Paulsen, K.D., Hoopes, P.J., Kennedy, F.E., Hartov, A., Roberts, D.W.: In vivo quantification of a homogenous brain deformation model for updating preoperative images during surgery. *IEEE Trans. Biomed. Eng.* **47**(2), 266–273 (2000)
39. Wittek, A., Omori, K.: Parametric study of effects of brain-skull boundary conditions and brain material properties on responses of simplified finite element brain model under angular acceleration in sagittal plane. *JSME Int. J.* **46**(4), 1388–1398 (2003)
40. Wittek, A., Kikinis, R., Warfield, S.K., Miller, K.: Brain shift computation using a fully non-linear biomechanical model. In: *8th International Conference on Medical Image Computing and Computer Assisted Surgery MICCAI 2005*. Palm Springs (2005)
41. Wittek, A., Hawkins, T., Miller, K.: On the unimportance of constitutive models in computing brain deformation for image-guided surgery. *Biomech. Model. Mechanobiol.* **8**, 77–84 (2009)
42. Dutta-Roy, T., Wittek, A., Miller, K.: Biomechanical modelling of Normal pressure hydrocephalus. *J. Biomech.* **41**(10), 2263–2271 (2008)
43. Mostayed, A., Garlapati, R.R., Joldes, G.R., Wittek, A., Kikinis, R., Warfield, S.K., Miller, K.: Intraoperative update of neuro-images: comparison of performance of image warping using patient-specific biomechanical model and BSpline image registration. In: Wittek A., Miller K., Nielsen P.M.F. (eds) *Computational Biomechanics for Medicine: Models, Algorithms and Implementation*, pp. 127–141. Springer, New York (2013)
44. Hu, J., Jin, X., Lee, J.B., Zhang, L., Chaudhary, V., Guthikonda, M., Yang, K.H., King, A.I.: Intraoperative brain shift prediction using a 3D inhomogeneous patient-specific finite element model. *J. Neurosurg.* **106**, 164–169 (2007)
45. Joldes, G.R., Wittek, A., Miller, K.: Suite of finite element algorithms for accurate computation of soft tissue deformation for surgical simulation. *Med. Image Anal.* **13**(6), 912–919 (2009)
46. Joldes, G.R., Wittek, A., Miller, K., Morriss, L.: Realistic and efficient brain-skull interaction model for brain shift computation. In: *Computational Biomechanics for Medicine III Workshop, MICCAI*. New-York (2008)
47. Yin, Z., Hughes, J.D., Glaser, K.J., Manduca, A., Van Gompel, J., Link, M.J., Romano, A., Ehman, R.L., Huston 3rd, J.: Slip interface imaging based on MR-elastography preoperatively predicts meningioma-brain adhesion. *J. Magn. Reson. Imaging.* **46**(4), 1007–1016 (2017)
48. Jin, X.: *Biomechanical Response and Constitutive Modeling of Bovine Pia-Arachnoid Complex*. Wayne State University, Detroit, Michigan, USA (2009)
49. Agrawal, S., Wittek, A., Joldes, G.R., Bunt, S., Miller, K.: Mechanical properties of brain-skull interface in compression. In: Doyle, B.J., Miller, K., Wittek, A., Nielsen, P.M.F. (eds.) *Computational Biomechanics for Medicine: New Approaches and New Applications*, pp. 83–91. Springer, New York (2015)

50. Mazumder, M.M.G., Miller, K., Bunt, S., Mostayed, A., Joldes, G., Day, R., Hart, R., Wittek, A.: Mechanical properties of the brain–skull interface. *Acta Bioeng. Biomech.* **15**(2), 9 (2013)
51. Wang, F., Han, Y., Wang, B., Peng, Q., Huang, X., Miller, K., Wittek, A.: Prediction of brain deformations and risk of traumatic brain injury due to closed-head impact: Quantitative analysis of the effects of boundary conditions and brain tissue constitutive model. *Biomech. Model. Mechanobiol.* (2018). <https://doi.org/10.1007/s10237-018-1021-z>
52. Miller, K., Lu, J.: On the prospect of patient-specific biomechanics without patient-specific properties of tissues. *J. Mech. Behav. Biomed. Mater.* **27**, 154–166 (2013)
53. McAnearney, S., Fedorov, A., Joldes, G., Hata, N., Tempany, C., Miller, K., Wittek, A.: The effects of Young’s Modulus on predicting prostate deformation for MRI-guided interventions. In: *Computation Biomechanics for Medicine V. The Workshop affiliated with Medical Image Computing and Computer Assisted Intervention Conference MICCAI 2010. Beijing (2010)*
54. Miller, K.: Constitutive modelling of abdominal organs (Technical note). *J. Biomech.* **33**, 367–373 (2000)
55. Bilston, L.E. (ed.): *Neural Tissue Biomechanics. Studies in Mechanobiology, Tissue Engineering and Biomaterials.* Springer, Berlin (2011)
56. Miller, K.: Method of testing very soft biological tissues in compression. *J. Biomech.* **38**, 153–158 (2005)
57. Miller, K.: How to test very soft biological tissues in extension. *J. Biomech.* **34**(5), 651–657 (2001)
58. Ferrant, M., Nabavi, A., Macq, B., Jolesz, F.A., Kikinis, R., Warfield, S.K.: Registration of 3-D intraoperative MR images of the brain using a finite-element biomechanical model. *IEEE Trans. Med. Imaging.* **20**, 1384–1397 (2001)
59. Warfield, S.K., Haker, S.J., Talos, F., Kemper, C.A., Weisenfeld, N., Mewes, A.U.J., Goldberg-Zimring, D., Zou, K.H., Westin, C.F., Wells III, W.M., Tempany, C.M.C., Golby, A., Black, P.M., Jolesz, F.A., Kikinis, R.: Capturing intraoperative deformations: research experience at Brigham and Women’s Hospital. *Med. Image Anal.* **9**(2), 145–162 (2005)
60. Fung, Y.C.: *A First Course In Continuum Mechanics*, p. 301. Prentice-Hall, London (1969)
61. Ciarlet, P.G.: *Mathematical Elasticity: Three-Dimensional Elasticity*, vol. 1. North Holland, The Netherlands (1988)
62. Nowinski, W.L.: Modified Talairach Landmarks. *Acta Neurochir.* **143**, 1045–1057 (2001)
63. Miller, K., Wittek, A.: Neuroimage registration as displacement - zero traction problem of solid mechanics (lead lecture). In: *Computational Biomechanics for Medicine MICCAI-associated Workshop. MICCAI, Copenhagen (2006)*
64. Bathe, K.-J.: *Finite Element Procedures.* Prentice-Hall, Englewood Cliffs (1996)
65. Dumpuri, P., Thompson, R.C., Dawant, B.M., Cao, A., Miga, M.I.: An atlas-based method to compensate for brain shift: preliminary results. *Med. Image Anal.* **11**(2), 128–145 (2007)
66. Dutta Roy, T.: *Does Normal Pressure Hydrocephalus have Mechanistic Causes?* The University of Western Australia, Perth (2010)
67. Tavner, A., Roy, T.D., Hor, K.W.W., Majimbi, M., Joldes, G.R., Wittek, A., Bunt, S., Miller, K.: On the appropriateness of modelling brain parenchyma as a biphasic continuum. *J. Mech. Behav. Biomed. Mater.* **61**, 511–518 (2016)
68. Miller, K., Chinzei, K.: Constitutive modelling of brain tissue: experiment and Theory. *J. Biomech.* **30**, 1115–1121 (1997)
69. Miller, K., Chinzei, K.: Mechanical properties of brain tissue in tension. *J. Biomech.* **35**, 483–490 (2002)
70. Mendis, K.K., Stalnaker, R.L., Advani, S.H.: A constitutive relationship for large deformation finite element modeling of brain tissue. *J. Biomech. Eng.* **117**, 279–285 (1995)
71. Miller, K.: Constitutive modelling of abdominal organs. *J. Biomech.* **33**, 367–373 (2000)
72. Miller, K., Chinzei, K., Orsengo, G., Bednarz, P.: Mechanical properties of brain tissue in vivo: experiment and computer simulation. *J. Biomech.* **33**, 1369–1376 (2000)
73. Miller, K.: Constitutive model of brain tissue suitable for finite element analysis of surgical procedures. *J. Biomech.* **32**, 531–537 (1999)

74. Nasser, S., Bilston, L.E., Phan-Thien, N.: Viscoelastic properties of pig kidney in shear, experimental results and modelling. *Rheol. Acta.* **41**, 180–192 (2002)
75. Bilston, L., Liu, Z., Phan-Tiem, N.: Large strain behaviour of brain tissue in shear: some experimental data and differential constitutive model. *Biorheology.* **38**, 335–345 (2001)
76. Farshad, M., Barbezat, M., Flüeler, P., Schmidlin, F., Graber, P., Niederer, P.: Material characterization of the pig kidney in relation with the biomechanical analysis of renal trauma. *J. Biomech.* **32**(4), 417–425 (1999)
77. Walsh, E.K., Schettini, A.: Calculation of brain elastic parameters in vivo. *Am. J. Phys.* **247**, R637–R700 (1984)
78. Miller, K., Chinzei, K.: Mechanical properties of brain tissue in tension. *J. Biomech.* **35**, 483–490 (2002)
79. Bilston, L.E., Liu, Z., Phan-Tien, N.: Linear viscoelastic properties of bovine brain tissue in shear. *Biorheology.* **34**(6), 377–385 (1997)
80. Miller, K.: *Biomechanics of the Brain for Computer Integrated Surgery*. Publishing House of Warsaw University of Technology, Warsaw (2002)
81. Prange, M.T., Margulies, S.S.: Regional, directional, and age-dependent properties of the brain undergoing large deformation. *ASME J. Biomech. Eng.* **124**, 244–252 (2002)
82. Seo, J., Kim, Y.-s.: Ultrasound imaging and beyond: recent advances in medical ultrasound. *Biomed. Eng. Lett.* **7**(2), 57–58 (2017)
83. Dietrich, C.F., Cantisani, V.: Current status and perspectives of elastography. *Eur. J. Radiol.* **83**(3), 403–404 (2014)
84. Sinkus, R., Tanter, M., Xydeas, T., Catheline, S., Bercoff, J., Fink, M.: Viscoelastic shear properties of in vivo breast lesions measured by MR elastography. *Magn. Reson. Imaging.* **23**, 159–165 (2005)
85. McCracken, P.J., Manduca, A., Felmlee, J., Ehman, R.L.: Mechanical transient-based magnetic resonance elastography. *Magn. Reson. Med.* **53**(3), 628–639 (2005)
86. Green, M.A., Bilston, L.E., Sinkus, R.: In vivo brain viscoelastic properties measured by magnetic resonance elastography. *NMR Biomed.* **21**(7), 755–764 (2008)
87. Glaser, K.J., Manduca, A., Ehman, R.L.: Review of MR elastography applications and recent developments. *J. Magn. Reson. Imaging.* **36**(4), (2012)
88. Murphy, M.C., Huston 3rd, J., Ehman, R.L.: MR elastography of the brain and its application in neurological diseases. *NeuroImage.* **187**, 176–183 (2019, Feb)
89. Bathe, K.J.: *Finite Element Procedures*. Prentice-Hall, Inc., Upper Saddle River (1996)
90. Ma, J., Wittek, A., Singh, S., Joldes, G., Washio, T., Chinzei, K., Miller, K.: Evaluation of accuracy of non-linear finite element computations for surgical simulation: study using brain phantom. *Comput. Methods Biomech. Biomed. Eng.* **13**(6), 783–794 (2010)
91. Wittek, A., Dutta-Roy, T., Taylor, Z., Horton, A., Washio, T., Chinzei, K., Miller, K.: Subject-specific non-linear biomechanical model of needle insertion into brain. *Comput. Methods Biomech. Biomed. Eng. J.* **11**(2), 135–146 (2008)
92. Garlapati, R., Roy, A., Joldes, G., Wittek, A., Mostayed, A., Doyle, B., Warfield, S., Kikinis, R., Knuckey, N., Bunt, S., Miller, K.: More accurate neuronavigation data provided by biomechanical modeling instead of rigid registration. *J. Neurosurg.* **120**(6), 1477–1483 (2014)
93. Mostayed, A., Garlapati, R.R., Joldes, G.R., Wittek, A., Roy, A., Kikinis, R., Warfield, S.K., Miller, K.: Biomechanical model as a registration tool for image-guided neurosurgery: evaluation against BSpline registration. *Ann. Biomed. Eng.* **41**(11), 2409–2425 (2013)
94. Warfield, S.K., Haker, S.J., Talos, I.-F., Kemper, C.A., Weisenfeld, N., Mewes, U.J., Goldberg-Zimring, D., Zou, K.H., Westin, C.-F., Wells, W.M., Tempny, C.M.C., Golby, A., Black, P.M., Jolesz, F.A., Kikinis, R.: Capturing intraoperative deformations: research experience at Brigham and Women’s hospital. *Med. Image Anal.* **9**(2), 145–162 (2005)
95. Joldes, G.R., Wittek, A., Miller, K.: An adaptive dynamic relaxation method for solving nonlinear finite element problems. Application to brain shift estimation. *Int. J. Numer. Methods Biomed. Eng.* **27**(2), 173–185 (2011)
96. Wittek, A., Miller, K., Kikinis, R., Warfield, S.K.: Patient-specific model of brain deformation: application to medical image registration. *J. Biomech.* **40**(4), 919–929 (2007)

97. Wittek, A., Joldes, G., Couton, M., Warfield, S.K., Miller, K.: Patient-specific non-linear finite element modelling for predicting soft organ deformation in real-time; application to non-rigid neuroimage registration. *Prog. Biophys. Mol. Biol.* **103**(2–3), 292–303 (2010)
98. Wittek, A., Hawkins, T., Miller, K.: On the unimportance of constitutive models in computing brain deformation for image-guided surgery. *Biomech. Model. Mechanobiol.* **8**(1), 77–84 (2009)
99. Joldes, G.R., Wittek, A., Miller, K.: Non-locking tetrahedral finite element for surgical simulation. *Commun. Numer. Methods Eng.* **25**(7), 827–836 (2009)
100. Grosland, N.M., Shivanna, K.H., Magnotta, V.A., Kallemeyn, N.A., DeVries, N.A., Tadepalli, S.C., Lisle, C.: IA-FEMesh: an open-source, interactive, multiblock approach to anatomic finite element model development. *Comput. Methods Prog. Biomed.* **94**(1), 96–107 (2009)
101. Joldes, G.R., Wittek, A., Miller, K.: Cortical surface motion estimation for brain shift prediction. In: Miller, K., Nielsen, P.M.F. (eds.) *Computational Biomechanics for Medicine*, pp. 53–62. Springer, New York (2010)
102. Miller, K., Lu, J.: On the prospect of patient-specific biomechanics without patient-specific properties of tissues. *J. Mech. Behav. Biomed. Mater.* **27**, 154 (2013)
103. Joldes, G.R., Wittek, A., Miller, K., Morriss, L.: Realistic and efficient brain-skull interaction model for brain shift computation. In: Miller, K., Nielsen, P.M.F. (eds.) *Computational Biomechanics for Medicine III*. Springer, New York (2008)
104. Wittek, A., Omori, K.: Parametric study of effects of brain-skull boundary conditions and brain material properties on responses of simplified finite element brain model under angular acceleration impulse in sagittal plane. *JSME Int. J.* **46**(4), 1388–1399 (2003)
105. Joldes, G.R., Wittek, A., Couton, M., Warfield, S.K., Miller, K.: Real-time prediction of brain shift using nonlinear finite element algorithms. In: Yang, G.Z., Hawkes, D., Rueckert, D., Nobel, A., Taylor, C. (eds.) *Medical Image Computing and Computer-Assisted Intervention - Miccai 2009, Pt II*, pp. 300–307. Springer, Berlin/Heidelberg (2009)
106. Miller, K., Chinzei, K.: Mechanical properties of brain tissue in tension. *J. Biomech.* **35**(4), 483–490 (2002)
107. Sinkus, R., Tanter, M., Xydeas, T., Catheline, S., Bercoff, J., Fink, M.: Viscoelastic shear properties of in vivo breast lesions measured by MR elastography. *Magn. Reson. Imaging.* **23**(2), 159–165 (2005)
108. Joldes, G.R., Wittek, A., Miller, K.: Suite of finite element algorithms for accurate computation of soft tissue deformation for surgical simulation. *Med. Image Anal.* **13**(6), 912–919 (2009)
109. Miller, K., Joldes, G., Lance, D., Wittek, A.: Total Lagrangian explicit dynamics finite element algorithm for computing soft tissue deformation. *Commun. Numer. Methods Eng.* **23**(2), 121–134 (2007)
110. Miller, K., Joldes, G.R., Bourantas, G., Warfield, S.K., Hyde, D.E., Kikinis, R., Wittek, A.: *Biomechanical Modeling and Computer Simulation of the Brain during Neurosurgery*. arXiv:1904.01192 (2019)
111. Joldes, G.R., Wittek, A., Miller, K.: Computation of intraoperative brain shift using dynamic relaxation. *Comput. Methods Appl. Mech. Eng.* **198**(41–44), 3313–3320 (2009)
112. ABAQUS: *ABAQUS 6.14 Documentation*. Rhode Island, USA (2018)
113. Fedorov, A., Billet, E., Prastawa, M., Gerig, G., Radmanesh, A., Warfield, S.K., Kikinis, R., Chrisochoides, N.: Evaluation of brain MRI alignment with the Robust Hausdorff Distance Measures. In: Bebis, G. (ed.) *Advances in Visual Computing, Pt I*, pp. 594–603 (2008)
114. Canny, J.: A computational approach to edge detection. *IEEE Trans. Pattern Anal. Mach. Intell.* **8**(6), 679–698 (1986)
115. Huttenlocher, D.P., Klanderman, G.A., Rucklidge, W.J.: Comparing images using the Hausdorff distance. *IEEE Trans. Pattern Anal. Mach. Intell.* **15**(9), 850–863 (1993)
116. Fedorov, A., Beichel, R., Kalpathy-Cramer, J., Finet, J., Fillion-Robin, J.C., Pujol, S., Bauer, C., Jennings, D., Fennessy, F., Sonka, M.: 3D slicer as an image computing platform for the quantitative imaging network. *Magn. Reson. Imaging.* **30**(9), 1323–1341 (2012)

117. Warfield, S.K., Haker, S.J., Talos, I.F., Kemper, C.A., Weisenfeld, N., Mewes, A.U.J., Goldberg-Zimring, D., Zou, K.H., Westin, C.F., Wells, W.M., Tempany, C.M.C., Golby, A., Black, P.M., Jolesz, F.A., Kikinis, R.: Capturing intraoperative deformations: research experience at Brigham and Women's Hospital. *Med. Image Anal.* **9**(2), 145–162 (2005)
118. Nakaji, P., Spetzler, R.F.: Innovations in surgical approach: the marriage of technique, technology, and judgment. *Clin. Neurosurg.* **51**, 177–185 (2004)
119. Oden, J.T., Belytschko, T., Babuska, I., Hughes, T.J.R.: Research directions in computational mechanics. *Comput. Methods Appl. Mech. Eng.* **192**, 913–922 (2003)
120. Taylor, Z., Miller, K.: Reassessment of brain elasticity for analysis of biomechanisms of hydrocephalus. *J. Biomech.* **37**, 1263–1269 (2004)
121. Miller, K., Taylor, Z., Nowinski, W.L.: Towards computing brain deformations for diagnosis, prognosis and neurosurgical simulation. *J. Mech. Med. Biol.* **5**(1), 105–121 (2005)
122. Berger, J., Horton, A., Joldes, G., Wittek, A., Miller, K.: Coupling finite element and mesh-free methods for modelling brain deformations in response to tumour growth. In: *Computational Biomechanics for Medicine III MICCAI-Associated Workshop*. MICCAI, New York City (2008)
123. Zienkiewicz, O.C., Taylor, R.L.: *The Finite Element Method*. Mcgraw-Hill Book Company, London (2000)